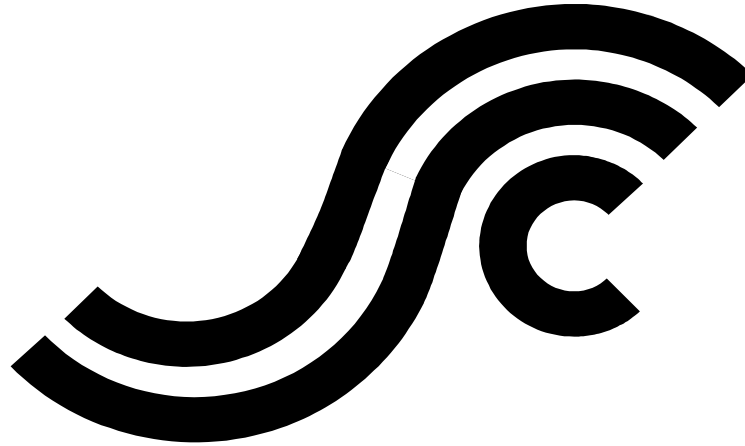**SSC – 479**

LOCALIZED WELD REPAIR OF ALUMINUM STRUCTURES BY LOW-HEAT INPUT PROCESSES

**Ship
Structure
Committee**

2025

This page intentionally left blank

**Ship
Structure
Committee**

SSC – 479
SR – 1484

LOCALIZED WELD REPAIR OF ALUMINUM STRUCTURES BY LOW-HEAT INPUT PROCESSES

Aluminum alloys, particularly the 5XXX series, are increasingly used in maritime applications due to their favorable strength-to-weight ratio and good corrosion resistance in salt water. However, these alloys are prone to sensitization from Al-Mg intermetallic compounds, leading to stress corrosion cracking, especially in saltwater environments. Welding exacerbates this issue, degrading mechanical and corrosion performance in the heat-affected zones.

This study performed a technology survey to identify appropriate repair methodologies for shipbuilding and ship repair applications, with a focus on the use of low heat input welding technologies to mitigate sensitization. The low heat input welding technology that was tested showed no significant improvement over conventional Gas Metal Arc Welding (GMAW) in reducing sensitization and resulted in lack of fusion defects. Alternative controlled waveform welding processes available outside the scope of this study are recommended for future study as potential candidates for low heat input welding of aluminum for maritime applications.

We thank the authors and Project Technical Committee for their dedication and research toward completing the objectives and tasks detailed throughout this paper and continuing the Ship Structure Committee's mission to enhance the safety of life at sea.

W. R. ARGUIN
Rear Admiral, U.S. Coast Guard
Co-Chairman, Ship Structure Committee

P. D. SMALL
Rear Admiral, U.S. Navy
Co-Chairman, Ship Structure Committee

SHIP STRUCTURE COMMITTEE

PROJECT TECHNICAL COMMITTEE

The Ship Structure Committee greatly appreciates the contributions of the individuals that volunteered their time to participate on the Project Technical Committee, listed below, and thanks them heartily. They were the subject matter expert representatives of the Ship Structure Committee to the contractor, performing technical oversight during contracting, advising the contractor in cognizant matters pertaining to the contract of which the agencies were aware, and performing technical peer review of the work in progress and upon completion.

Chair:

LCDR Carol Yin, U.S. Coast Guard

Members:
Dr. Dongchun Qiao, American Bureau of Shipping
Ms. Tayyebe Seif, Transport Canada
Mr. Tao Xu, Ship Structures Consultant
Mr. Kayode Oyedemi, American Bureau of Shipping
Mr. John McGrorey, NAVSEA
Dr. Jonah Klemm-Toole, Colorado School of Mines
Mr. Rong Huang, Ship Structures Consultant
Ms. Jeannette Viernes, Military Sealift Command

Ship Structure Committee Executive Director:
LCDR Bryan Andrews, U.S. Coast Guard

1. Report No. SSC-479	2. Government Accession No.	3. Recipient's Catalog No.
4. Title and Subtitle Localized Weld Repair of Aluminum Structures by Low-heat Input Processes		5. Report Date 3 June 2025
		6. Performing Organization Code

7. Author(s)
  Kim Tran
  Rachel Mooar
  Mackenzie Perry
  Andrew Lo
  Justin Norkett
		8. Performing Organization Report No.
		    SR-1484

9.Performing Organization Name and Address The Welding, Processing, and Nondestructive Evaluation (NDE) Naval Surface Warfare Center Carderock Division (NSWCCD)		10. Work Unit No. (TRAIS)
		11. Contract or Grant No.
12. Sponsoring Agency Name and Address Ship Structure Committee C/O US Coast Guard 2703 Martin Luther King Jr. Ave. SE Washington, DC 20593-7509		13. Type of Report and Period Covered Final Report
		14. Sponsoring Agency Code CG-5PS
15. Supplementary Notes		

16. Abstract

Aluminum alloys, particularly the 5XXX series, are increasingly utilized in maritime applications due to their favorable strength-to-weight ratio and good corrosion resistance in saltwater environments. However, these alloys are prone to sensitization, where highly reactive Al-Mg intermetallic compounds precipitate along grain boundaries, leading to stress corrosion cracking. This issue is exacerbated by welding, which degrades the mechanical and corrosion performance in the heat-affected and fusion zones. The Naval Surface Warfare Center Carderock Division (NSWCCD) investigated low heat input welding technologies to mitigate sensitization during ship repair. The Fronius Cold Metal Transfer (CMT) system was tested against conventional Gas Metal Arc Welding (GMAW). Comparative studies revealed no significant improvement in sensitization with CMT, and the technique resulted in a higher occurrence of lack of fusion defects.

17. Key Words Aluminum Alloys, Sensitization, Mechanical Testing	18. Distribution Statement Approved for public release; distribution is unlimited. Available from: National Technical Information Service Springfield, VA 22161 (703) 487-465	

19. Security Classif. (of this report)
          Unclassified
	20. Security Classif. (of this page)
	             Unclassified
		21. No. of Pages
		    44
			22. Price

CONVERSION FACTORS
(Approximate conversions to metric measures)

To convert from	to	Function	Value
LENGTH			
inches	meters	divide	39.3701
inches	millimeters	multiply by	25.4000
feet	meters	divide by	3.2808
VOLUME			
cubic feet	cubic meters	divide by	35.3149
cubic inches	cubic meters	divide by	61,024
SECTION MODULUS			
inches^2 feet	centimeters^2 meters	multiply by	1.9665
inches^2 feet	centimeters^3	multiply by	196.6448
inches^3	centimeters^3	multiply by	16.3871
MOMENT OF INERTIA			
inches^2 feet^2	centimeters^2 meters^2	divide by	1.6684
inches^2 feet^2	centimeters^4	multiply by	5993.73
inches^4	centimeters^4	multiply by	41.623
FORCE OR MASS			
long tons	tonne	multiply by	1.0160
long tons	kilograms	multiply by	1016.047
pounds	tonnes	divide by	2204.62
pounds	kilograms	divide by	2.2046
pounds	Newtons	multiply by	4.4482
PRESSURE OR STRESS			
pounds/inch^2	Newtons/meter^2 (Pascals)	multiply by	6894.757
kilo pounds/inch^2	mega Newtons/meter^2 (mega Pascals)	multiply by	6.8947
BENDING OR TORQUE			
foot tons	meter tons	divide by	3.2291
foot pounds	kilogram meters	divide by	7.23285
foot pounds	Newton meters	multiply by	1.35582
ENERGY			
foot pounds	Joules	multiply by	1.355826
STRESS INTENSITY			
kilo pound/inch^2 inch$^{1/2}$(ksi√in)	mega Newton MNm$^{3/2}$	multiply by	1.0998
J-INTEGRAL			
kilo pound/inch	Joules/mm^2	multiply by	0.1753
kilo pound/inch	kilo Joules/m^2	multiply by	175.3

CONTENTS

FIGURES

TABLES

1. EXECUTIVE SUMMARY

Due to their favorable strength to weight ratio, aluminum alloys are often used as structural materials in maritime applications. The 5XXX series alloys have been of particular interest due to generally good corrosion resistance in salt water applications. However, these alloys are subject to sensitization due to the precipitation of highly reactive Al-Mg intermetallic compounds both in service and due to even short heating cycles. These precipitates form contiguous networks along grain boundaries which can cause significant stress corrosion cracking, particularly in the salt water environments these alloys operate in. As a result, welding results in significant degradation of the mechanical and corrosion performance within the heat-affected and fusion zones of welds made during fabrication and repair of aluminum vessels.

The Welding, Processing, and Nondestructive Evaluation (NDE) branch of Naval Surface Warfare Center Carderock Division (NSWCCD) investigated alternate technologies for fusing aluminum plate structures for ship repair applications. Low heat input welding technologies were chosen as the primary focus of this work under the hypothesis that less heating of the material during welding would result in a smaller degree of sensitization than conventional welding technologies.

A survey of existing low heat input welding technologies was performed and the Fronius Cold Metal Transfer (CMT) system was chosen for further testing. Based on a comparative study of the electrochemical and mechanical response of CMT and conventional Gas Metal Arc Welding (GMAW), no significant improvement was observed with respect to the sensitization produced between the two techniques. Furthermore, the low heat input of the CMT technique resulted in a higher occurrence of lack of fusion defects during joining.

While tests with Fronius CMT technology indicate that there are concerns with subsurface defects, there are alternative controlled waveform welding processes available outside the scope of this study that may be potential candidates for low heat input welding of aluminum for maritime applications. In addition, exploration of non-arc welding technologies such as handheld laser welding is recommended for future study.

2. BACKGROUND

Aluminum alloys in maritime environments are susceptible to various forms of degradation, depending on the specific environmental conditions encountered over the service life of the material and the alloy series. Despite the concerns associated with material degradation, the use of aluminum alloys for maritime applications has steadily increased due to the lightweight strength and low cost of aluminum [1].

5XXX series (Al-Mg) alloys are non-heat treatable binary alloys that derive their strength from solid solution strengthening and strain hardening. Al-Mg alloys containing more than 3.0 weight percent Mg can develop a susceptible microstructure or become sensitized when exposed to elevated temperatures (>120°F) for a prolonged period of time [2] [3] [4]. Sensitization results from the formation of a continuous network of β-phase (Al_3Mg_2) at the grain boundaries [2] [3] [4]. The β-phase is anodic to the adjacent metal matrix, thus the grain boundaries become highly susceptible to stress corrosion cracking (SCC) and intergranular corrosion cracking (IGC). Effective repair methods for sensitized 5XXX-series aluminum alloy is a critical consideration for the ship repair industry, as SCC can significantly affect the seaworthiness of aluminum vessels.

Sensitization is defined as an aging process, whether accidental, intentional, or incidental (as during welding), that causes precipitation of constituents at grain boundaries. Temperatures between 100°F and 150°F can cause sensitization for 5XXX series aluminum alloys containing more than 3.0 weight percent Mg within months. The amount of Mg and the amount of strain hardening can lengthen the exposure time required for sensitization to occur. If the metal is heated to temperatures between 300°F and 400°F, formation of precipitates at the grain boundary can occur within hours [5]. Thus, undesired sensitization may occur during welding. Exposure to elevated welding temperatures can result in formation of a continuous network of β-phase precipitates along the Heat-Affected Zone (HAZ) and weld metal [6] [7] [8].

5XXX-series aluminum alloys are subject to a loss of strength during welding due to the thermal cycles of heating and cooling. The thermal effects of welding results in the annealing of the HAZ. The stages of annealing include recovery, recrystallization, and grain growth; as a result, annealing alters the microstructure and eliminates the strength benefits derived from strain hardening.

2.1 Assessment and Repair of Sensitized 5XXX-Series Aluminum Alloys

Sensitization of 5XXX-series aluminum alloys is assessed using the ASTM G67 Nitric Acid Mass Loss Test (NAMLT). This test classifies the degree of sensitization (DoS) in the terms of mg/cm^2 of material lost following exposure of a test specimen to nitric acid at 86°F for 24 hours [1]. A DoS level of <30 mg/cm^2 is considered to be weldable, 30-60 mg/cm^2 is considered to be moderately sensitized and weldable with surface treatment (cold working), and >60 mg/cm^2 is considered highly sensitized and un-weldable [1]. Material with a NAMLT result of <20 mg/cm^2 is considered un-sensitized, with a mass loss >20 mg/cm^2 considered the onset of sensitization. These categories and classifications, used by the US Navy, are based on extensive experience with weld repair of sensitized 5XXX-series aluminum material in CG-47 class and LCS class applications, and may not be applicable to other vessel types and service conditions.

Cracks in sensitized 5XXX-series aluminum alloys are typically repaired by the use of insert plates – the cracked area and a surrounding portion of the base material is removed and replaced with a suitable insert welded into place. Direct weld repair (e.g. excavation of the crack and refill with sound weld metal) is limited to materials with low levels of sensitization due to the tendency for sensitized base material to crack when exposed to the thermal cycles and residual stresses of welding. On moderately sensitized material, techniques designed to induce compressive stresses in the metal, such as Ultrasonic Impact Technology (UIT) and Laser Surface Peening (LSP), can be applied to successfully facilitate welding by reducing the likelihood of crack propagation during welding [1].

2.2 Current Weld Repair Technologies

Welding of aluminum is typically performed using a gas-shielded welding process. The two most common welding methods in the ship repair industry are GMAW and GTAW [9]. The primary welding method in the aluminum ship industry is conventional GMAW which can result in relatively high heat inputs (typically in excess of 25 kJ/in). GTAW can produce even higher heat inputs (typically in excess of 30 kJ/in) than those experienced during GMAW but is typically limited to very small repairs. This motivates investigation into lower heat input welding technologies in order to mitigate the strength losses in 5XXX-series.

GMAW is a semiautomatic welding process wherein an automatically fed, continuous, consumable electrode shielded by an externally supplied gas is utilized [10]. This process is considered semiautomatic, as once the parameters are set on the welding machine, the welder only controls travel speed, travel direction, and gun position. The welding equipment performs automatic self-regulation of the welding arc characteristics (e.g. arc voltage and wire feed speed/current) to control all other aspects of welding [10].

The electrical characteristic of the welding arc influences the mode of metal transfer. By the definitions of the American Welding Society (AWS), there are three modes of metal transfer [10]. These are short-circuiting transfer, globular metal transfer, and spray transfer. Note that one variation of spray transfer is specifically identified as Gas Metal Arc Welding Pulsed Spray Transfer (GMAW-P), and that there are various welding equipment manufacturers that have proprietary variations on the three metal transfer modes.

Gas Metal Arc Welding Short-Circuiting Transfer (GMAW-S) encompasses the lowest range of welding currents and electrode diameters associated with GMAW [10]. Transfer of metal occurs during the physical contact and short circuiting of the welding electrode with the base material, with no transfer of metal across the welding arc. This creates a weld pool that is relatively small and fast-freezing compared to other modes of metal transfer. As such, GMAW-S is generally suited for joining of thin sections, out-of-position welding, and bridging large root gaps [10]; however, it must be noted that conventional and unmodified GMAW-S is poorly suited for the welding of aluminum due to the risk of incomplete fusion and porosity [10]. As the overall energy transfer is relatively low, GMAW-S is considered a relatively low heat input process.

The globular mode of metal transfer involves the transfer of molten metal in the form of large droplets across the welding arc as opposed to a short circuiting, direct-contact mechanism [10]. These globules of molten weld metal are relatively large, characteristically larger in diameter than the consumable electrode, and are acted upon by gravity. As this process is gravity dependent, it tends to restrict globular transfer to the flat position. Similar to GMAW-S, conventional globular transfer has significant risks of incomplete fusion and excessive porosity in the resultant weld, and is not recommended for the welding of aluminum [9]. No further discussion will take place with regard to the globular transfer mode, as it is not often used in welding of aluminum.

The remaining mode of metal transfer is the spray transfer mode, which is also known as the axial spray transfer mode. In this mode of metal transfer, the welding current is above a critical value termed the spray transition current [10]. Below this threshold, metal transfer occurs in the globular manner; above it, there is enough energy in the welding arc to drive small droplets of molten metal with sufficient force to overcome gravity. This allows limited out of position welding, but primarily allows the smooth, splatter-free transfer of filler material to the weld. The deeply penetrating arc produced by the high welding currents required to function in the spray transfer mode inhibit welding on thinner materials. In addition, the high deposition rate may be prohibitive for out-of-position welding due to the large weld pools produced [10].

GMAW-P is a modification of GMAW in the spray transfer mode designed to overcome the position and thickness limitations of spray transfer, relying on an engineered and precisely controlled waveform and frequency that "pulses" the welding current and voltage [10]. Two levels of current are provided; one is a background current that maintains the welding arc, while the other is a superimposed pulse of current that drives metal transfer. During this pulse, one or more drops are formed and transferred; the frequency and the amplitude of the pulses control the energy level of the arc and therefore the rate at which the wire melts [10]. GMAW-P allows lower relative heat inputs compared to conventional GMAW in the spray transfer mode.

Shipbuilders and ship repair facilities typically rely on GMAW in the spray transfer mode as well as GMAW-P for fabrication and repair welding of aluminum alloys. These processes offer the optimum combination of weld quality as well as speed of welding. However, GMAW in the spray transfer mode has one of the highest heat inputs possible, and GMAW-P, while a lower average heat input than GMAW in the spray transfer mode, still possesses relatively high heat input [10]. As such, alternative technologies must be explored in order to reduce the heat input and limit the overall thermal effects of welding on 5XXX-series.

2.3 Low Heat Input Welding Technologies

Welding equipment manufacturers have developed various proprietary GMAW-S modes in order to reduce heat input during welding to facilitate a reduction in distortion caused by welding, as well as enabling the welding of thinner material with lower risk of burn-through, reduced splatter, and a reduction in other welding-related defects [11].

For the purposes of this technology survey, these proprietary technologies and processes have been grouped as Controlled Waveform Low Heat Input (CWLHI) techniques. CWLHI equipment has been produced by multiple Original Equipment Manufacturers (OEMs), relying on various proprietary engineered waveforms to produce the desired low heat input during welding. The vast majority of these processes rely on hardware or software control of the welding current during modified GMAW-S; a selection of these technologies and OEMs is provided in Table 1 [11].

Note that at least one OEM has developed a modified GMAW-P mode. This allows additional options for low heat input welding. However, while discussion of this process is included in this survey for completeness, the modified GMAW-P technology is not being considered further at this point in order to evaluate the various GMAW-S processes under consideration.

Table 1. OEM Controlled Waveform Low Heat Input Processes **[11]**.

Manufacturer's Name	Manufacturer's Process
ESAB	Qset
EWM	coldArc
Fronius	Cold Metal Transfer (CMT)
Fronius	Pulse Multi Control (PMC) [1]
Kemppi	Wise Series
Lincoln Electric	Surface Tension Transfer (STT)
Merkle	ColdMIG
Miller Electric	Regulated Metal Deposition (RMD)

[1] Note that Fronius PMC is a combined GMAW-S and GMAW-P process

2.4 Manufacturer's Welding Technology Claims and Evaluation

What follows is a listing of each technology and the claims made by their respective OEM:

ESAB QSet – This technology monitors the short-circuiting process and adjusts arc voltage as required to maintain an optimal burn-off rate, in order to provide a more consistent heat input and reduce the amount of spatter produced during welding [12]. Note that this technology appears to be a European regional item, as no references to QSet have been identified in the literature for ESAB North America.

EWM coldArc – This technology claims to be a "heat-reduced, low-spatter short arc for high dimensional stability welding" [13]. Little additional information is available regarding this particular process.

Fronius CMT – This technology is unique in the modified GMAW-S realm, in that the control system detects the short-circuiting portion of metal transfer and uses a mechanical action within the welding gun to withdraw the weld wire before repositioning it to minimize the amount of heat input and spatter produced during welding [14].

Fronius PMC – This technology is, as previously noted, a combined GMAW-S and GMAW-P process. The addition of a wire control system in the form of a penetration stabilizer, as well as the presence of an arc length stabilizer, directly influences the process' ability to weld with reduced spatter and a highly stable, controlled arc [15].

Kemppi Wise series – This technology encompasses multiple software packages used in conjunction with the OEM's welding machines to provide controlled waveform and GMAW-S arc stability [16].

Lincoln STT – This technology is a controlled GMAW-S process. It relies on current controls to adjust heat input independently of wire feed speed, allowing reduced spatter and lower heat input while welding [17].

Merkle ColdMIG – This technology relies on control of the welding current during the up and down-slow cycles using a digital signal processor. By sharply controlling current, heat input is reduced during welding [18].

Miller RMD – This technology is a modified GMAW-S process, specifically optimized for the welding of stainless-steel pipe. It accomplishes this by anticipating and controlling the short-circuiting portion of metal transfer, reducing current after the short to create consistent transfer [19].

Of the eight processes identified in the industry survey above, seven are modifications of the conventional GMAW-S process, and one is a modification of GMAW-P and GMAW-S. These processes will be evaluated based on availability, design intent (e.g. program optimization), and other parameters to identify a candidate process for further investigation.

Fronius PMC shall be disregarded for the purposes of this evaluation, as the intent is to compare various modified GMAW-S processes. Of the remainder, Miller RMD and Lincoln Electric STT are disregarded as they are optimized for work on ferrous materials; ESAB QSet is disregarded due to product non-availability within North America; and EWM coldArc, the Kemppi Wise software series, and Merkle ColdMIG are disregarded due to the anticipated difficulties in procuring European welding equipment.

As such, this leaves Fronius CMT as the down-selected test candidate for CWLHI welding of thin aluminum for ship repair applications. This down-selection is accomplished on the basis of technology availability as well as the optimization for welding of aluminum alloys.

3. APPROACH

3.1 Test Plan Development

A test plan was developed to identify and coordinate the required nondestructive and destructive testing. Four candidate base material and filler material combinations were identified for further work, although two of the proposed material combinations were eliminated near the end of the project due to workload constraints. A description of the reduction in scope of this project will be provided in **Appendix A** of this report. The two combinations which were investigated were: (1) unsensitized grade 5456-H116 plate welded with grade 5556 filler material, (2) laboratory-sensitized grade 5456-H116 plate welded with grade 5556 filler material.

Grade 5456-H116 plate in accordance with ASTM B928 [20] was procured in 0.250" thicknesses. These plates were procured from Pierce Aluminum, dual-certified to ASTM B928 grade 5456-H116 and grade 5456-H321 specifications. These plates arrived at NSWCCD in 8'x4' plates and were subsequently mechanically sheared to provide smaller test plates. Five types of test plates were created for this test program, including deep-V and shallow-V simulated fatigue crack repair areas, large and small corrosion repair areas, as well as a large number of V-groove butt joint weldments for mechanical test specimens.
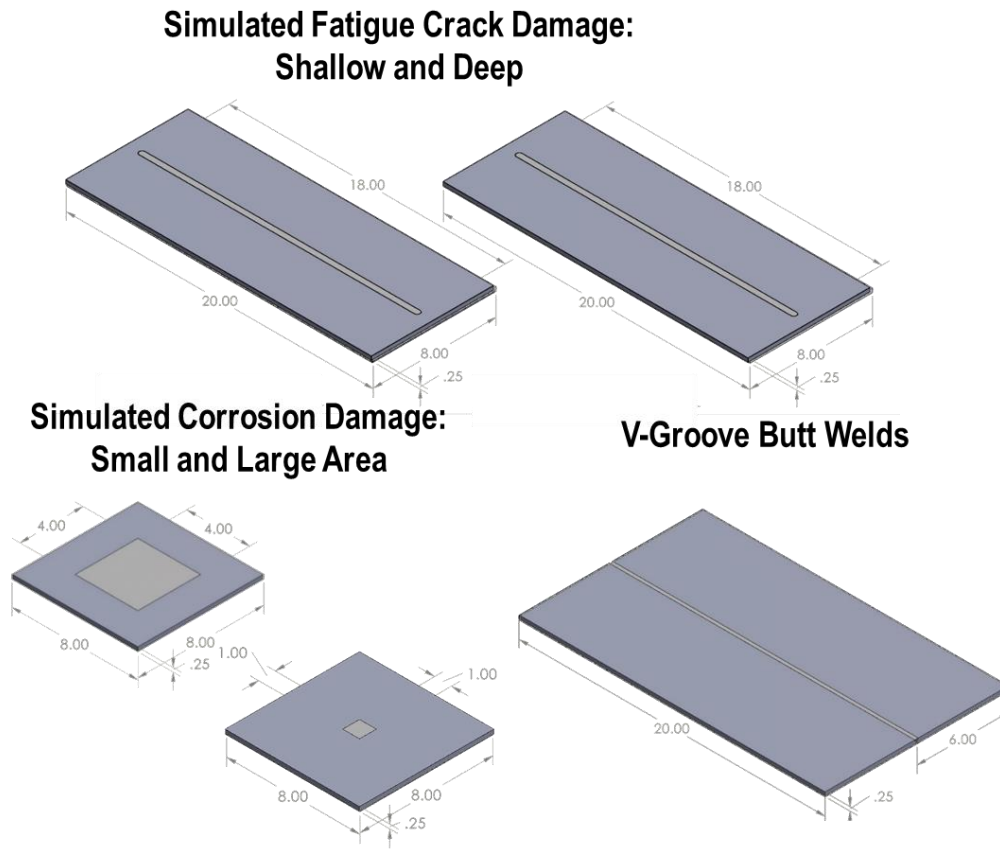
Figure 1. Geometries of the test articles used in this study.

The test plan called for metallography, ASTM G67 NAMLTs, procedure qualification testing (bend tests and tensile tests), electrochemical testing, fatigue testing, and fracture toughness testing on both sensitized and unsensitized plates welded with the CMT process. However, due to constraints in funding as well as availability of test equipment, the planned testing was significantly down scoped. The final test plan is listed in **Table 2** below.

Table 2. Executed test plan for this program. Numbers represent the number of specimens produced and tested.

	AA5456 (Unsensitized)		AA5456 (Sensitized)	
Material	**CMT**		**CMT**	
	Base	**Weld**	**Base**	**Weld**
Bend Test				3
Tensile Test				2
G67 NAMLT	2	2	2	2
OCP + CYPOL			3	3
Potentiostatic			3	3
Mixed Potentiostatic				3
Fatigue (air)				8
Fatigue (Seawater)				16
DC/PD Single-Edge Notch				2

3.2 Welding Procedure Development

Grade 5456-H116 aluminum was selected due to its higher strength compared to other grade 5xxx aluminum alloys used in maritime applications. This higher strength is due to the higher magnesium content of the alloy, and results in a higher susceptibility to corrosion. The –H116 temper was specifically selected, as it is the "marine grade" aluminum, with specific requirements in ASTM B928 regarding exfoliation corrosion resistance and intergranular corrosion resistance. However, it must be noted that these tests are specific for the wrought product in the as-purchased condition, and the resultant test data cannot be extended to material in the shipboard condition.

For the purposes of this study, the available grade 5456-H116 material was divided into two lots of prepared plates. Of these, one lot was left in the as-received condition, and the other lot was subjected to laboratory sensitization under controlled conditions. The sensitized lot of material was placed in a heating chamber and kept at 100°C for 28 days, with a pause at 7 days to assess the degree of sensitization and to determine the sensitization trend.

Evaluation of the available welding equipment at NSWCCD indicated that the existing Fronius welding machine, a TPS 320i, was not equipped to perform CMT welding due to lacking the required software unlock as well as the appropriate wire feeding system and push-pull gun. A delay in fabrication of the test weldments occurred while a Fronius system with CMT capability, an appropriate wire feeder, and a push-pull gun was obtained from Norfolk Naval Shipyard (NNSY). The specific system, a Fronius TransPuls Syneric CMT 3200 and accompanying CR 7000-CMT wire feeder, was borrowed from Code 138, Welding Engineering Division, at NNSY.

Upon delivery of the Fronius welding machine, NSWCCD personnel engaged in troubleshooting of the Fronius system, as the equipment was not in regular use at NNSY and required maintenance and replacement parts prior to restoring functionality. The NSWCCD welding technician specifically noted that the wire feeding process, especially through the push-pull gun, was difficult compared to conventional GMAW equipment, and that contact with Fronius technical support was required to set the system up. Once initial troubleshooting and preventative maintenance was completed, the technician reported that the equipment was operator-friendly and ran reliably with the exception of one wire feeding issue that was attributed to the spool of welding electrode as opposed to the welding machine or wire feeder.

3.3 Mechanical Testing Procedures

Procedure qualification record (PQR) testing in the form of bend and tensile testing was performed by IMR Test Labs in Lansing, NY. The specimens used for this testing were taken from a lab-sensitized V-groove butt weldment which underwent nondestructive testing in the form of visual inspection (VT), dye penetrant inspection (PT), and phase array ultrasonic inspection (UT) prior to machining. Bend testing was performed to 180° on a 2.25-inch mandrel in accordance with AWS B4.0:2016 [21]. Tensile strength was measured according to ASTM E 8-22 [22]. Further mechanical characterization was performed at NSWCCD by four-point bend fatigue testing and slow rising stress-intensity testing in artificial seawater for stress corrosion cracking (SCC) (ASTM D1141 [23]).

3.3.1 Fatigue Testing

Four point bend fatigue tests were performed with the following procedure. Specimens were cut via water-jet from a lab-sensitized V-groove butt welded plate. The edges were broken with a file and finished with a fine grit paper to ensure that surface cracks did not form from machining. Specimens were measured, and if required, prepped for seawater. Seawater cells were cut from 250mL plastic bottles and sealed with Momentive RTV 108. Seawater used met ASTM D1141 [23] standard. Specimens were loaded into the fatigue test machine. A Sonntag SF-1U unit was used for testing as seen in **Figure 2**. This machine uses a pendulum weight and LVDT on an isolated platform to test samples in fully-reversed four-point bend fatigue at approximately 30 hertz. Data was recorded to the nearest 1,000 cycle upon specimen failure, or runout was denoted past ten million (10^7) cycles.

Figure 2. Sonntag SF-1U unit with seawater specimen loaded into machine.

3.3.2 Stress Corrosion Cracking Testing

Stress corrosion testing was carried out via the slow-rising stress intensity test. A direct current potential difference (dcPD) system was used to measure crack length every 30 seconds. These measurements are used to control a hydraulic load frame according to stress intensity ramp rate in active feedback control. The test specimen geometry utilized in this test is the single-edge notched tension (SENT) specimen. Following machining from a lab-sensitized V-groove weldment, the SENTs were cleaned in acetone followed by methanol, and then sonicated in deionized water baths for 15 minutes each. Gauge thickness and width was measured via physical caliper measurement, and the notch depth was obtained by taking the average of 3 measurements per side of the SENT reduced gauge section using an optical microscope.

All tests were conducted using a software controlled, servo-hydraulic machine operating in displacement control mode with clevis grips allowing free rotation of the SENT specimens. A fatigue precrack was initiated in the SENT specimens in laboratory air under a K_{max} of 5.46 ksi$\sqrt{}$in at a frequency (f) of 3 Hz and a stress ratio ($R = K_{min}/K_{max}$) of 0.2 to reach 14 mils crack length beyond the notch. The crack was extended to a final crack length (notch plus crack) of 20 mils via decreasing K protocol (K-shed) from a K_{max} of 5.46 ksi$\sqrt{}$in to 3.18 ksi$\sqrt{}$in at an R of 0.1 and f of 5 Hz. An initial hold was performed at 1 ksi load for 0.5-1 hour; this step ensures crack monitoring signal stability and stabilization of the Al-Mg open circuit potential (OCP). For potentiostat-controlled testing, polarization to the potential of interest may begin during this hold, which was -0.810 volts versus Ag/AgCl reference electrode ($V_{Ag/AgCl}$) (via a potentiostat). This step enables the development of a constant initial crack tip chemistry.

The SCC testing was performed via slow-rising stress intensity at a loading rate (dK/dt) of 1.82 ksi$\sqrt{}$in/hr (2.0 MPa$\sqrt{}$m/hr) until either K = 13.76 ksi$\sqrt{}$in or specimen failure followed by a hold at 13.76ksi$\sqrt{}$. The loading rate was selected based on prior work [24] in high strength alloys evaluating the influence of loading rate on environmental susceptibility, unpublished evaluations at NSWCCD and at the University of Virginia, as well as program timeline considerations. The hold value was determined based on reaching the fracture toughness value for the alloy/specimen geometry if no cracking were to occur.

3.4 Electrochemical Testing Procedures

For electrochemical testing to assess possible changes in the corrosion performance of AA5456 subjected to cold-metal transfer (CMT) welding, 21 1" x 1" samples were cut from an 8" x 8" plate of lab-sensitized AA5456 welded with the CMT technique in a 4" x 4" area in the center to simulate corrosion repair. Samples were cut from four areas corresponding to different locations that may have been affected by the welding process: (1) six samples from the bulk alloy closer to the edges of the plate, (2) three samples surrounding the weld that will be referred to as the heat-affected zone (HAZ), (3) six samples across the interface of the weld and HAZ, and (4) nine samples from within the weld. **Figure 3** depicts the various sections provided as samples for this testing. Of the samples provided, three samples from each area were used for the electrochemical tests.
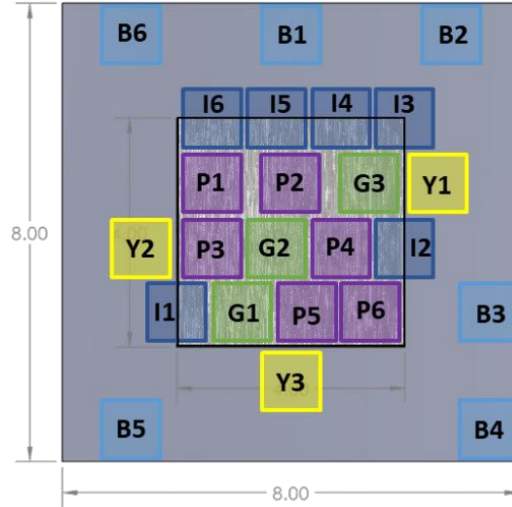
Figure 3. A schematic of samples sectioned from an AA5456 corrosion repair simulant plate with a cold-metal transfer welded region in the center. Samples labeled as bulk (BX) heat-affected (YX),weld (PX or GX), and weld/heat-affected zone interface (IX).

Open-circuit potential monitoring followed by anodic polarization measurements were conducted on nine of the samples corresponding to the bulk metal (area 1), HAZ (area 3), and the weld (area 4). These tests assess whether the fundamental corrosion properties, such as the open-circuit potential (OCP or E_{corr}), stabilization of the surface, steady state corrosion current (i_{corr}), anodic reaction kinetics, and pitting potential (E_{pit}), vary due to microstructural changes that could be caused by the CMT process. Three replicates were used from each area to account for some of this statistical variance. AA5XXX alloys have expected OCPs between -0.75 to -0.85 V vs a saturated calomel electrode (SCE) reference when immersed in seawater solutions, but this shows substantial stochastic variation and can even span a range of -0.65 to -0.9 V vs SCE [25] [26].

For these measurements, the 1" x 1" sample surfaces were ground to 600 grit with SiC paper and mounted with 1 cm^2 area exposed in an electrochemical cell using reference electrode and graphite rod counter-electrode. Samples were immersed in ASTM D1141 synthetic seawater (ASTM SW) for a 24 hr period where the OCP was monitored using a PARSTAT MC PMC-200 to allow the potential to stabilize as the initial surface film becomes modified by reactions with the exposure to ions within the seawater [27]. Following this period, an anodic scan was taken by measuring the current due to an applied voltage, starting at -25 mV vs. OCP and swept at +0.5 mV/s until the current density exceeds 1 mA/cm^2. The measurement of E_{corr} and i_{corr} was made using VersaStudio 2.61.2 software to perform a Tafel analysis, which fits a line to the approximately linear regions of the cathodic and anodic portions of the scan and uses the voltage and current value at the point where these lines intercept to determine those values.

Potentiostatic measurements were conducted on 12 of the samples, using three samples corresponding to each area. These tests are used to assess metastable pitting frequency as well as time to stable pitting, if stable pits do form over the test duration. By monitoring the current at a constant voltage, metastable pits can be detected by looking at points where the current spikes by >0.4 μA/cm^2 for at least 1.5 s before returning to a background level, and stable pitting can be

identified if the current spikes to values of 10 A/cm, judged by the current divided by the pit radius, without returning down to background [28]. For these measurements, the 1" x 1" samples surfaces were ground to 1200 grit with SiC paper, and a 1 cm^2 area was masked off with tape and chemical conversion coating applied to the surface around this area. This treatment is done to minimize the occurrence of crevice corrosion, which can invalidate the results of the measurement.

After treatment, the tape was removed from the sample and the samples were mounted with this 1 cm^2 area exposed in an electrochemical cell using an SCE reference electrode and graphite counter-electrode. Samples were immersed in ASTM SW for a 24 hr period to let the OCP stabilize. However, the OCP stabilizes but drifts about an average, and so the potentiostatic measurement consists of holding the voltage constant at the measured OCP for 25 min, followed by a five min interval to re-adjust the OCP and holding the voltage constant at this new value for 25 min more. This loop continued for an overall duration of five days or until a current density of 0.1 mA/cm^2 was reached.

4.   RESULTS AND DISCUSSION

The results of the laboratory sensitization treatments as measured by Nitric acid mass loss test (NAMLT) for each specimen are listed in **Table 3**. Despite a small deviation at the 7 day check, all three specimens produced a consistent degree of sensitization at 28 days. Weld parameter development, welder workmanship testing, and subsequent corrosion and mechanical testing was performed on test articles produced from material aged in this way.

Table 3. Nitric acid mass loss test (NAMLT) results for lab sensitized Grade 5456 Al specimens.

Sample ID	As-Received (mg/cm²)	7 Days (mg/cm²)	28 Days (mg/cm²)
Control	4.18	-	-
V-Groove 1-S	-	26.75	41.44
V-Groove 32-S	-	22.44	42.01
V-Groove 33-S	-	22.57	40.64

4.1 Welding Procedure Development

Extensive work was completed to optimize parameters for semi-automatic welding. Per the OEM, Fronius CMT is a process variation designed for robotic or mechanized welding rather than semi-automatic welding, and while it can be performed, it is not intended or designed for the application covered by this study. In addition, the OEM recommended that Fronius' PMC process be used for non-sheet-metal thicknesses of aluminum due to concerns with insufficient heat input and lack of fusion issues. The technician reported that the standard CMT process was indeed insufficient to ensure fusion in beads inside the groove weld geometries. However, due to procurement cost and the already-delayed test program, NSWCCD elected to continue with the CMT technology using the CMT Pulse process as a middle ground.

One issue noted by the welding technician was the significant distortion encountered during all phases of welding. While this is characteristic of welding thin aluminum plate, significant mitigating actions to counteract the effects of residual stress even at the relatively

lower heat inputs provided by the CMT process was required. It was specifically identified that stringer beads with a minimum of oscillation required for tie-in mitigated some of the distortion issues. In addition, a custom fixture was developed for welding the test plates. This involved backing using ceramic material along the root, as well as the use of multiple clamps to provide mechanical restraint for the test plates. It was additionally noted that even with optimized settings, distortion remained a concern for the duration of welding.

The selected welding parameters were optimized as shown in **Table 4**. It is noted that these welding parameters were developed under laboratory conditions, and that later destructive testing identified lack of fusion concerns in test plates. The test weldments successfully passed visual inspection and liquid penetrant inspection. As such, there remain potential issues associated with subsurface discontinuities when using the CMT welding process.

Table 4. Optimized parameters for the CMT process used to fabricate the test plates used in this work.

Program	CMT-5XXX
Wire Feed Speed	Set by program
Amperage	135
Voltage	19
Travel Speed	17-18 in/min
Torch Oscillation	Stringer

4.2 Nondestructive Testing

Visual (VT) and liquid penetrant (PT) inspection were carried out at NSWCCD on each of the V-Groove butt welds. It should be noted that this inspection was not performed by a Level II qualified inspector, though the procedures used were in compliance with NAVSEA TechPub T9074-AS-GIB-010/271 Rev 1 [29]. One of the test plates inspected in this way is shown in **Figure 4**. A close up image of the weld prior to coating with PT compounds is shown in **Figure 5**. Phased array ultrasonic inspection was performed on weldments prior to PQR testing. Neither visual and liquid penetrant testing nor phased array UT were able to identify any defects that caused concern in the PQR test weldment.
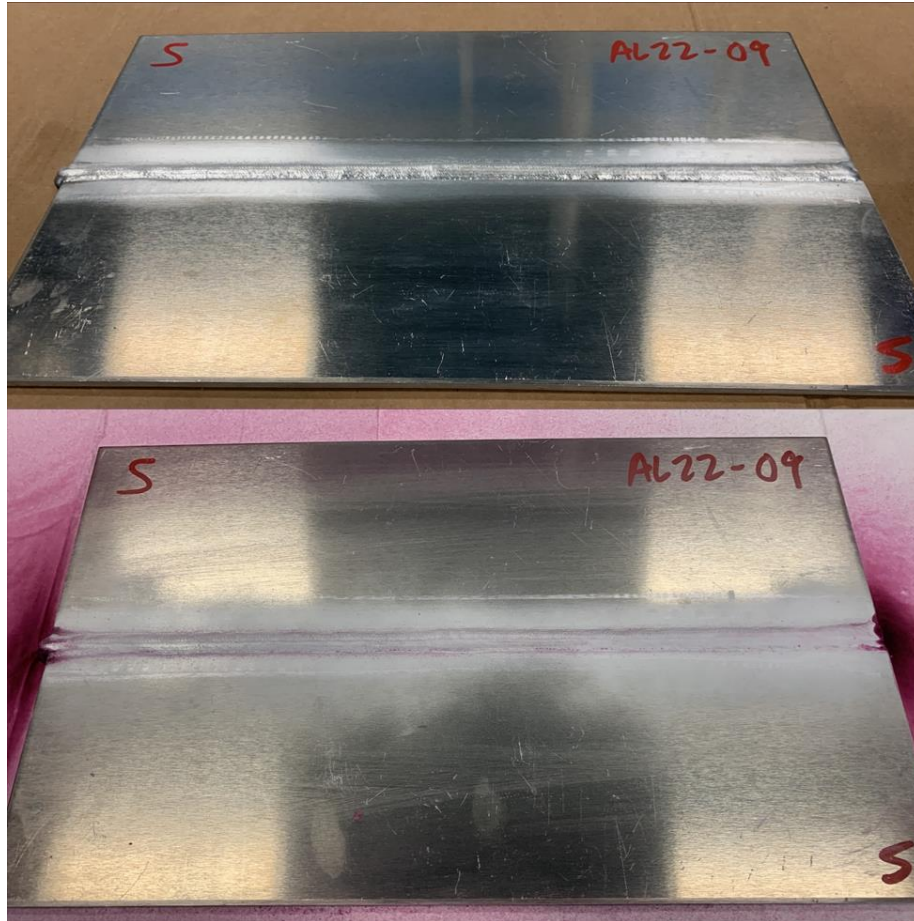
Figure 4. Test weldment used for PQR testing before and after visual and dye penetrant testing.
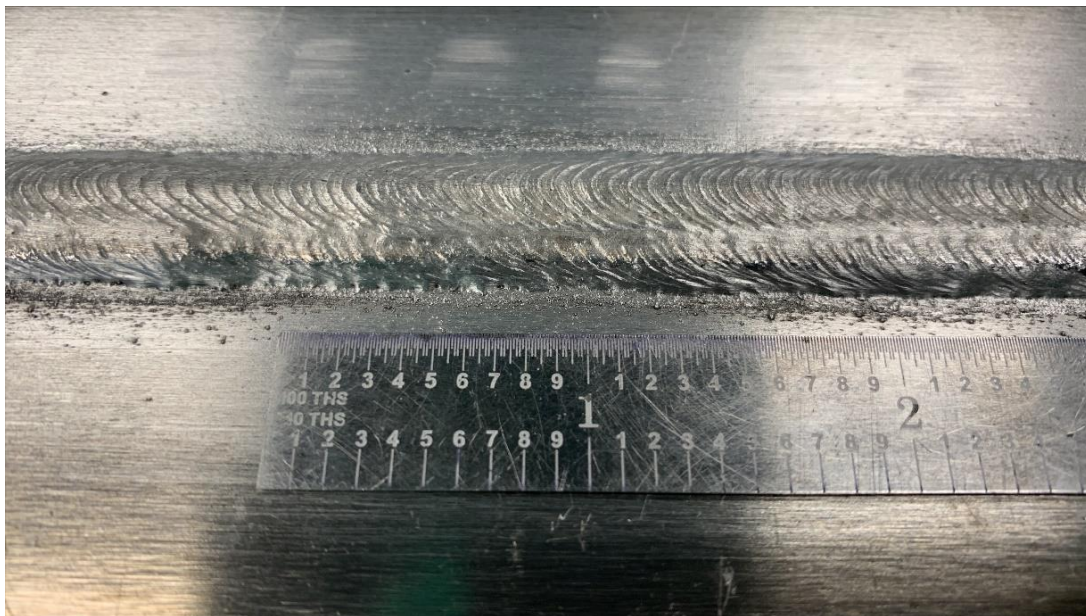
Figure 5. Close up photograph of one of the test weldments used for visual inspection.

Digital radiography was performed at Naval Air Station Patuxent River. An XRayWorx X-ray source was used with an operating voltage of 90 kV at 300 µA current. The tube to detector distance (FDD) was 1100 mm and the tube to object distance (FOD) was 728.9 mm. A number of porosity indications were observed with diameters between 0.01 and 0.03 inches, an example of which is shown in Error! Reference source not found..
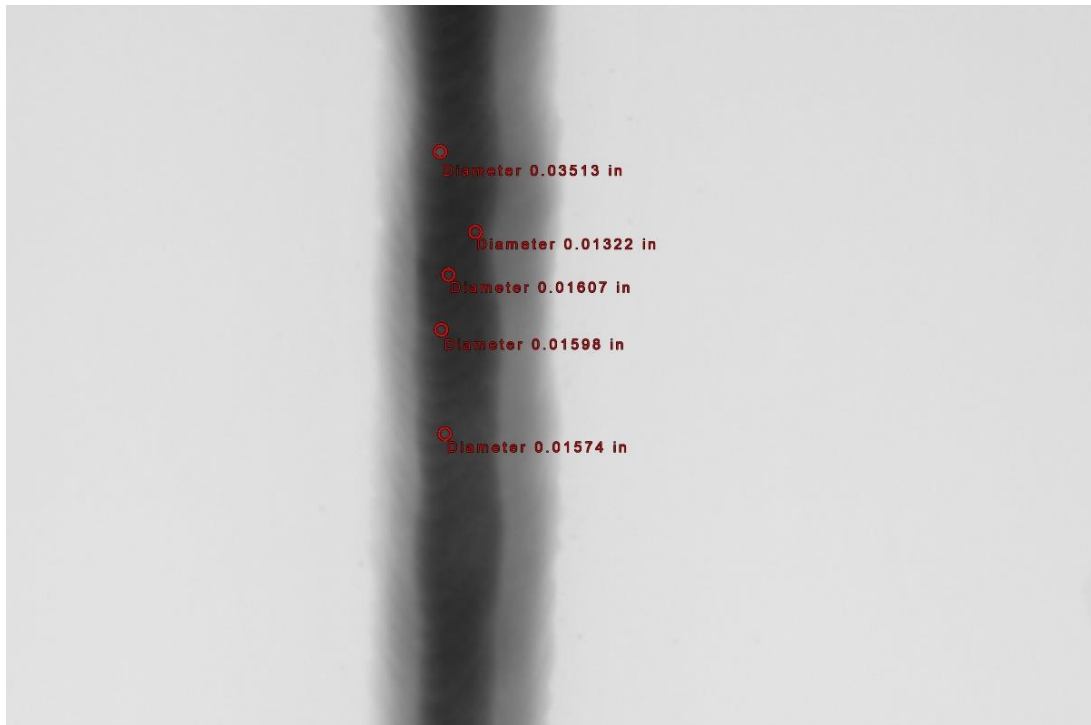
Figure 6. Digital radiography image showing indications in a lab sensitized grade 5456 aluminum weldment used for procedure qualification record (PQR) testing.

4.3 Metallography

Figure 7. Cross section of corrosion repair plate showing a large lack of fusion defect.

Weldments were sectioned to inspect the quality of the welds and any internal defects. Specimens were etched with phosphoric acid to reveal the precipitate phase that was developed during the sensitization treatment and subsequent welding. **Figure 7** is a composite image taken from a cross-sectional specimen from one of the large corrosion area repair specimens. This image was selected to note the subsurface lack of fusion. This defect occurred despite care taken during welding and in spite of the optimized welding parameters developed to support procedure qualification testing. Defects like this suggest that the low heat input of the CMT process can still result in lack of fusion. These defects are especially problematic in areas where inspection techniques such as visual, magnifier-assisted visual, and liquid penetrant inspection cannot detect discontinuities. Defects of this type that do not intersect the surface are not apparent in VT or PT inspection. The large void depicted in **Figure 8** shows another example of a pore on the order of indications detected in the digital radiography inspection described previously.

Figure 8. Porosity and large voids in a corrosion repair simulant plate.

Apparent in both **Figure 7Figure 8** is the degree of sensitization of the baseplates as revealed by the phosphoric acid etch. This etch attacks the Mg-rich beta precipitates along grain boundaries, producing a dark response which is apparent across all specimens. The abundance and continuity of the beta precipitate phase supports the findings of the NAMLT findings of sensitization in the base plates. **Figure 9** depicts the roots of a representative weldment (Fig. 9a) at progressively higher magnification. Porosity is apparent in both left and right weld roots and within the fusion zone (Fig. 9b and 9c), as well as a heightened precipitate etch response compared to the base metal. Closer examination of the right weld root (Fig. 9d) shows porosity at the interface as well as contiguous precipitation indicating apparent sensitization of the root.
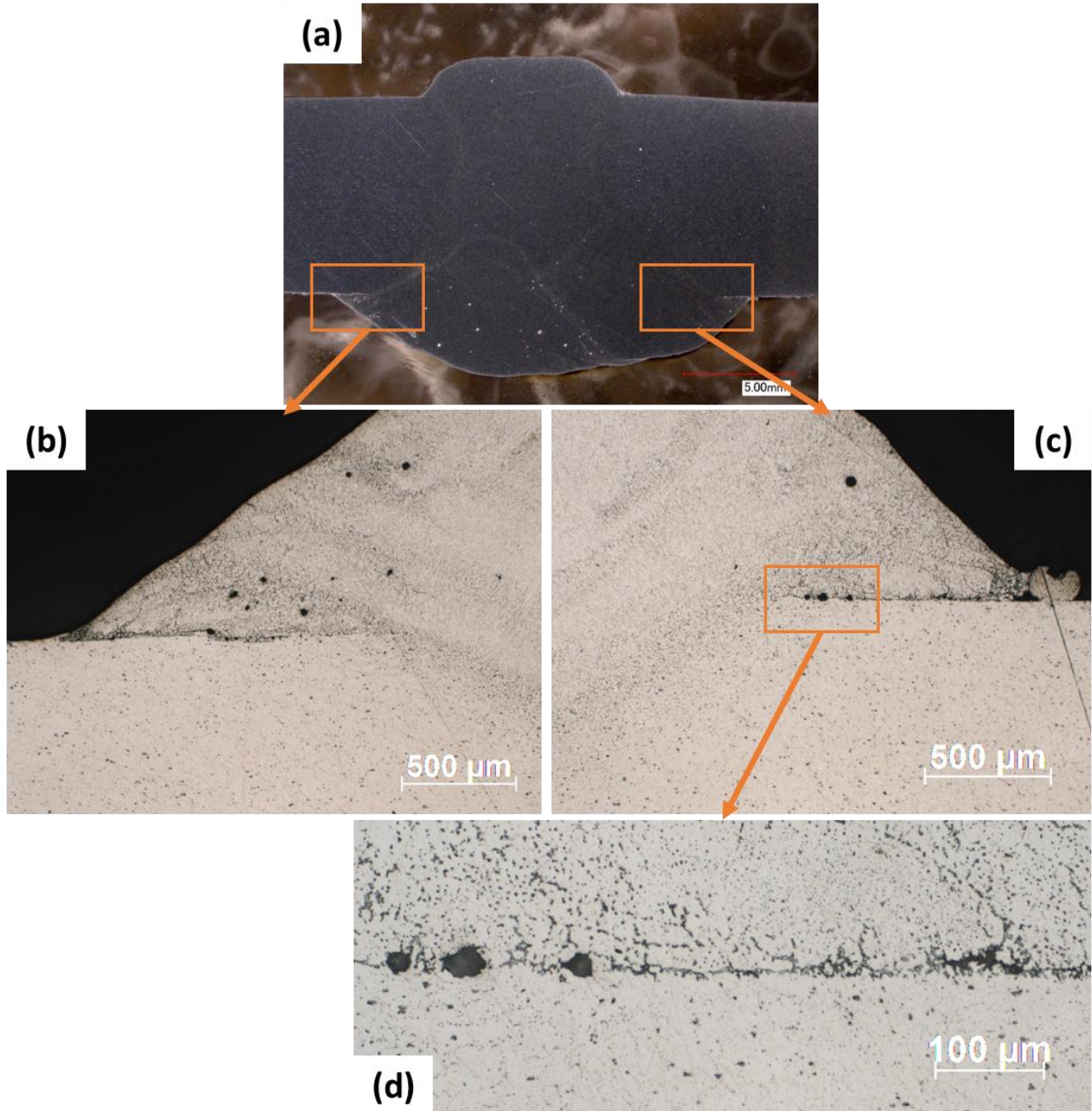
Figure 9. Metallography of the weld roots of one sensitized weldment (a) etched with phosphoric acid to reveal sensitization. Subfigures (b) and (c) show the left and right weld roots as indicated. Subfigure (d) shows a further magnified image of the fusion line of the right root.

4.4 Mechanical Testing

Specimens were tested by IMR Test Labs by bend and tensile testing for the procedure qualification record (PQR). No cracking was observed in the root or face of any weld specimens during bend testing to 180°. Tensile tests of two weldments found a tensile strength of 40.6 ksi (279.9 MPa) and 41.5 ksi (286.1 MPa) with failure occurring within the weld in both specimens.

4.4.1 Fatigue Testing
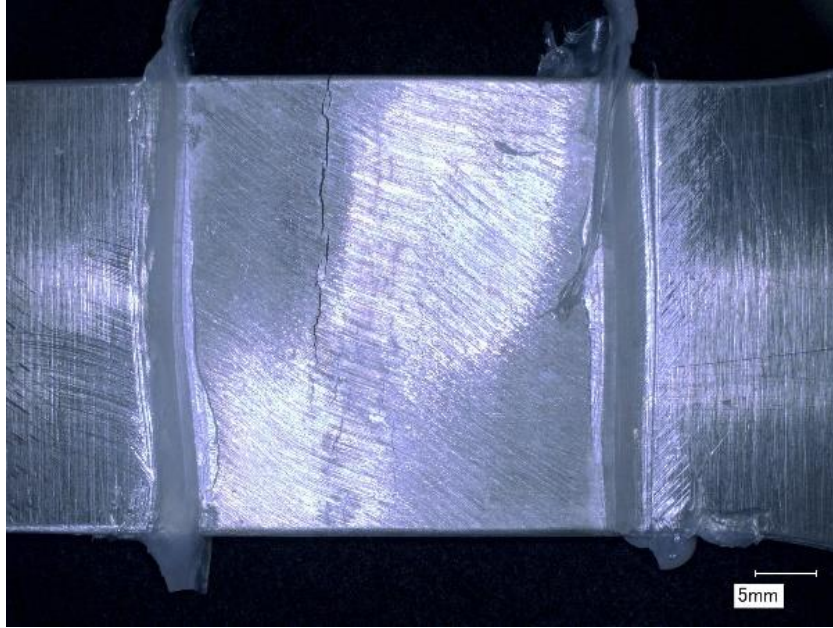
Figure 10. Fatigue failure for a specimen exposed to seawater.

Fatigue testing produced results expected of sensitized 5xxx series aluminum with a knock-down at all stress levels when testing in seawater. There was an approximately 3 times knock down in cycles to failure at 15 ksi. **Figure 11** shows the comparative fatigue performance in specimens exposed to seawater and air. Many specimens reached the runout condition and did not fail at 5 and 10 ksi load. For 10 ksi, it is impossible to know the true knockdown as most of the specimens in air were runouts and therefore did not fail. There would likely be a larger disparity in the curves had fatigue testing been conducted to a longer runout. Due to the limited failures and restricted stress ranges ASTM E739 cannot be accurately used to analyze these data trends. As a result, these results remain qualitative, however there was a definite reduction in fatigue performance in these specimens in seawater.
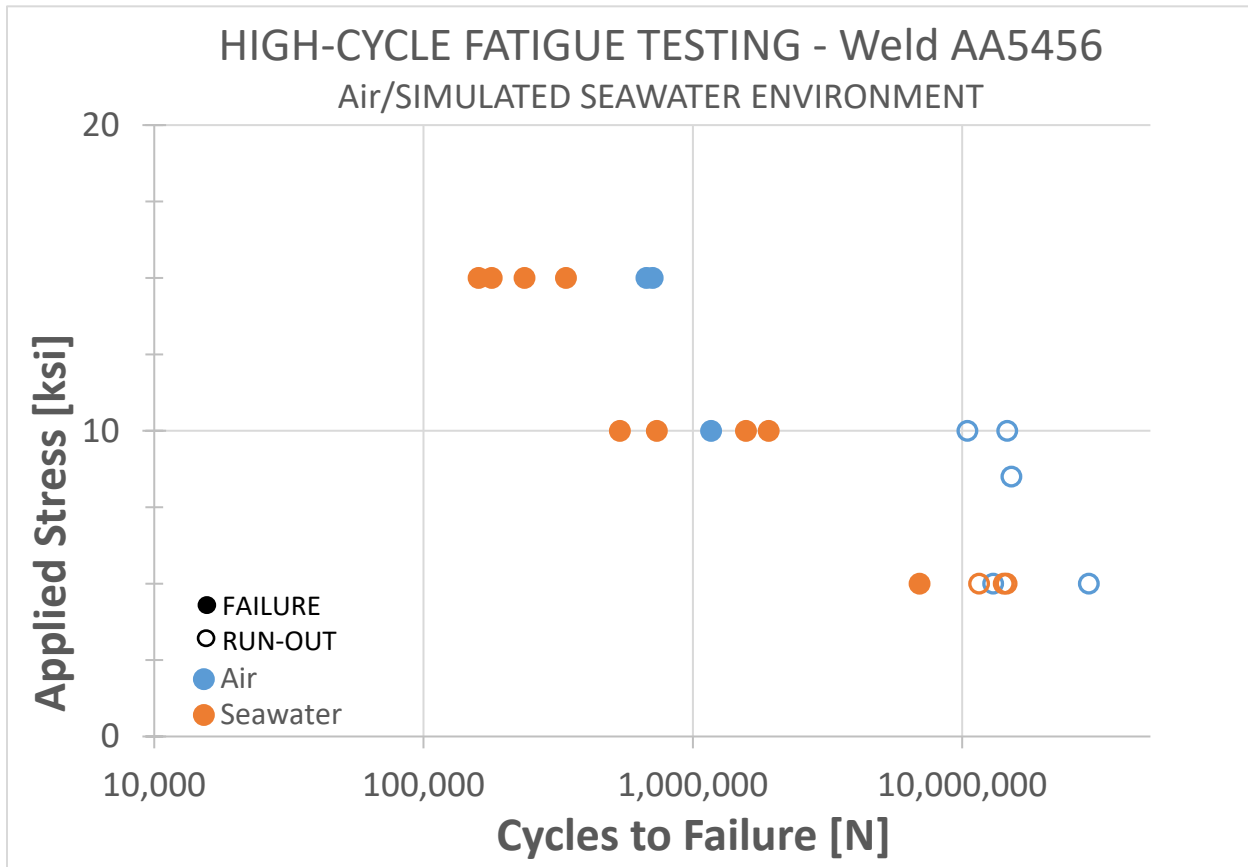
Figure 11. S-N curve for Welded 5456 aluminum in seawater and air.

The as-welded fatigue performance is consistent with previous studies using GMAW technology. Fatigue properties of the CMT-welded material are consistent with existing test data for welding of grade 5456-H116 aluminum shown in **Figure 12** [30]. This literature data demonstrates that even unsensitized 5456 Al plate is subject to a reduction in fatigue life in sea water. Welding with the conventional GMAW process results in a further loss relative to the plate form factor which is further exacerbated in sea water. These results demonstrate a similar sea water knockdown effect with the CMT process. However, further testing would be required in order to establish a quantitative and statistical comparison between the fatigue life of weldments produced between the two methods. Note that **Figure 12** below discusses grade 5456-H117 aluminum; upon consultation with the Aluminum Association, it was noted that the –H116 and –H117 tempers are equivalent, as they were manufacturer-proprietary tempers that were later consolidated into a single temper designated –H116.
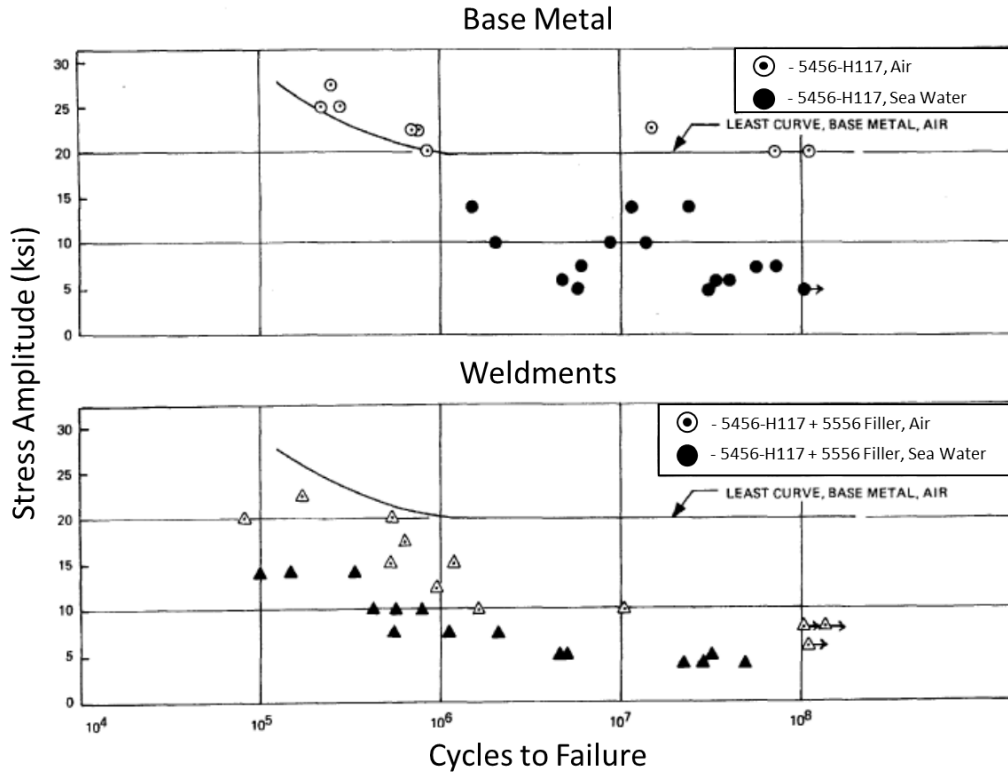
Figure 12. Fatigue curves for unsensitized 5456 aluminum base plate (top) and welds (bottom) in air and sea water. Adapted from [30].

4.4.2 Stress Corrosion Cracking Testing

Stress corrosion testing did not yield any conclusive results. Due to residual stress profile across the weld, face to root, a straight pre-crack could not be obtained with standard operating procedures. An example of a specimen with a pinned crack that resulted in poor data is shown in **Figure 13**. Further work would be required to develop a procedure to produce a suitable crack. However, given previous testing it is possible to say that stress corrosion cracking in the present orientation, normal to the transverse plate axis (T-L), is negligible [31]. Aluminum alloy 5456 is commonly cold rolled to increase strength which creates an anisotropic microstructure. Because of this anisotropy, the orientation of loading greatly increases (or decreases) the susceptibility of these metals to crack when exposed to seawater. See **Figure 14** for crack growth rate trends based on crack orientation.
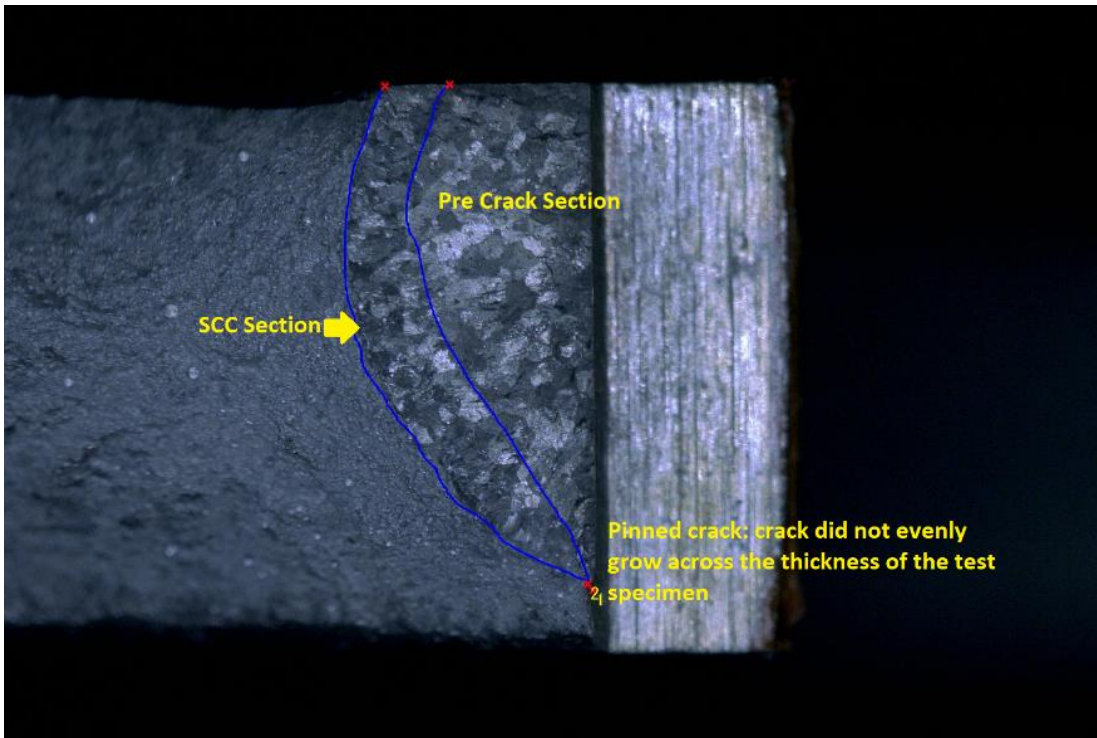
Figure 13. Pinned crack from a Welded SEN(T) specimen.
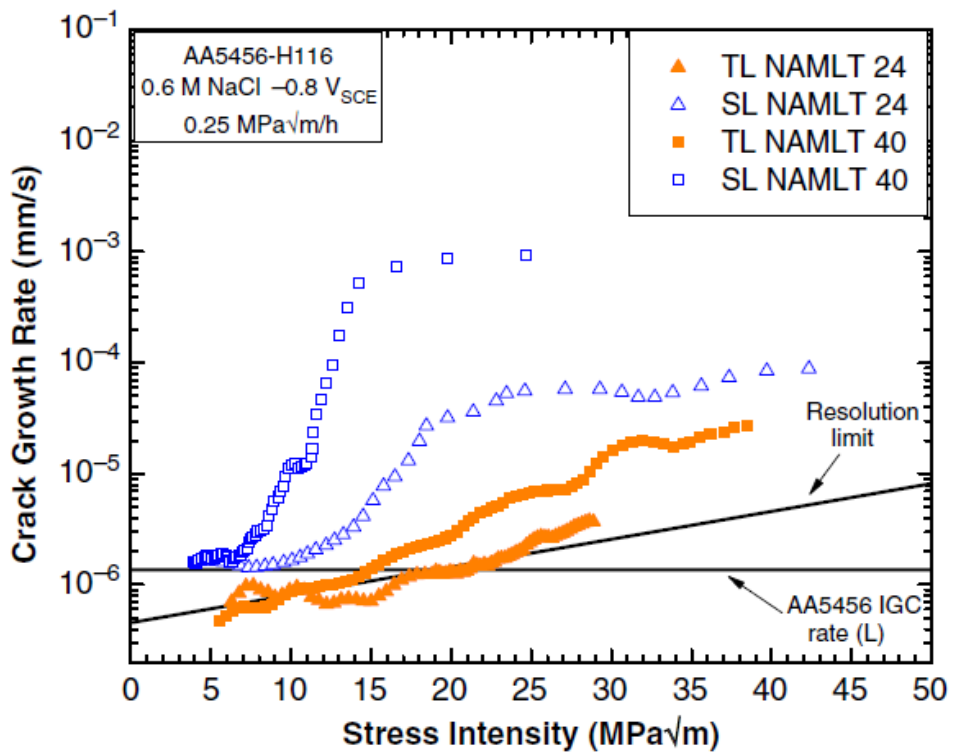
Figure 14. The effect of crack growth rate based on orientation in sensitized AA5456 **[31]**.

5. Electrochemical Testing

The measurements of open-circuit potential over a 24 hr immersion time are presented in **Figure 15**, with three plots broken out according by area of the plate samples were taken from: bulk metal (area 1, Fig. 15a), weld metal (area 4, Fig. 15b), and the HAZ (area 3, Fig.15c). For the bulk metal, it appears the surface stabilizes within the first 4 hrs of immersion, but the second sample shows some activity after 20 hrs of immersion causing the potential to start decreasing. The weld area samples show a more unstable OCP over the duration, with the second sample stabilizing close to 12 hrs of immersion, and the other two potentially stabilizing after 20 hrs. The HAZ samples show a mix between the results of the bulk and welded area, with initial
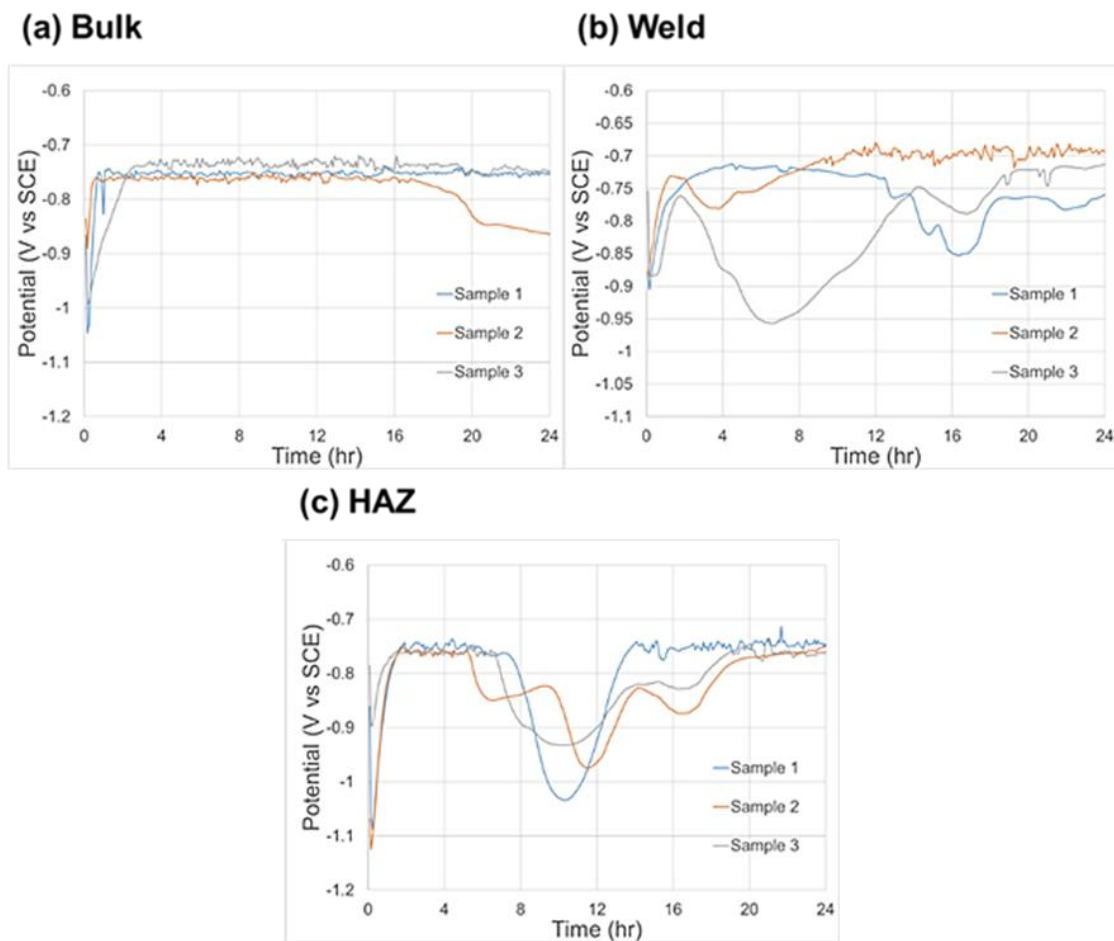
Figure 15. Open-circuit potential monitoring measurements taken for nine samples across three different areas of the welded plate: (a) bulk metal, (b) weld metal, and (c) the heat-affected zone (HAZ).

Anodic polarization curves for samples from the same areas as the OCP monitoring measurements are shown in **Figure 16** with Fig. 16a-c showing results for the bulk metal, weld metal, and HAZ areas, respectively. From these curves, parameters for E_{corr}, i_{corr}, E_{pit}, and ΔE_{bd} were extracted and are summarized in **Table 5**. The term ΔE_{bd} is determined by $E_{pit} - E_{corr}$, and it signifies the magnitude of the thermodynamic driving force for the stabilized

22

surface to experience breakdown and subsequently stable pitting. The curves visually demonstrate that both the bulk metal and HAZ areas had lower OCP values overall compared to the welded area, with average OCPs of -866, -843, and -742 mV vs SCE, respectively. Equilibrium corrosion current (i_{corr}) values were comparable between the three areas, showing a range of 22-81 nA/cm², with averages for the three areas coming out to 52, 45, and 63 nA/cm² between the bulk, welded, and HAZ areas, respectively. Pitting potentials (E_{pit}) were comparable across each area, with the welded and HAZ areas showing averages of -626 and -627 mV vs SCE compared to the average of -583 mV vs SCE for the bulk region.

However, the differences in ΔE_{bd} between regions, which provide the driving force for pitting, show the bulk areas with the largest difference of 283 mV compared to 217 mV for the HAZ and 117 mV for the welded area. This indicates the bulk metal has the least probable tendency to form stable pits, and this tendency increases moving towards the HAZ and then the welded area. Visually, the curves demonstrate metastable pitting events across some of the samples, judged by sudden horizontal spikes in current before the curve reaches E_{pit}. One such event can be seen on sample 1 of the bulk area. Several indications are seen on samples 1 and 2 of the welded area, and sample 2 of the HAZ shows some instability in metastable pitting right before E_{pit} on that curve.

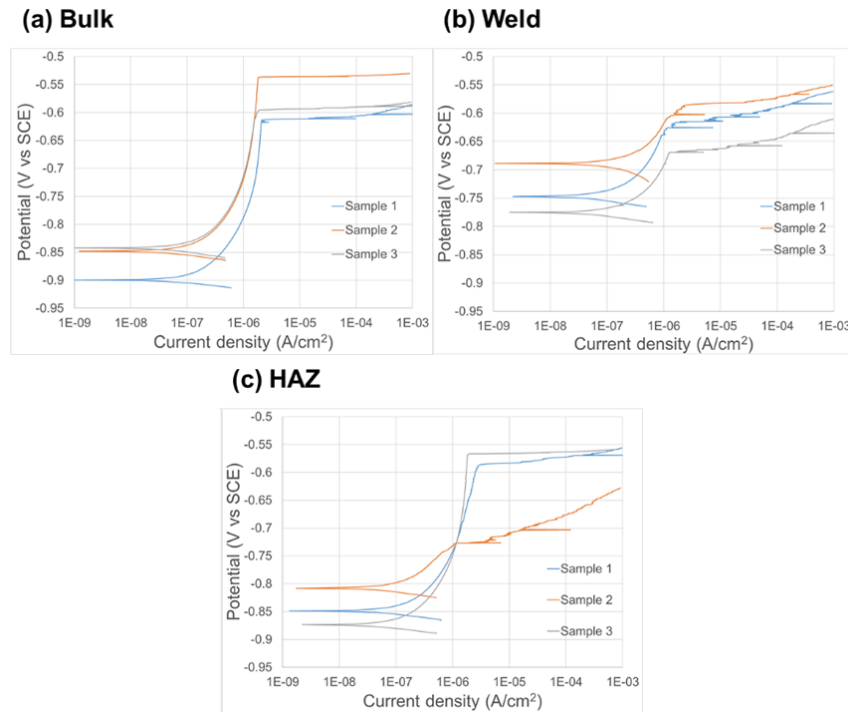**Figure 16.** Anodic polarization curves taken for nine samples across three different areas of the welded plate: (a) bulk metal, (b) weld metal, and (c) the heat-affected zone (HAZ).

Table 5. A summary of electrochemical properties extracted from anodic polarization curves of 9 samples taken from different areas across the welded plate.

Area	Sample	E_{corr} (mV vs SCE)	E_{pit} (mV vs SCE)	ΔE_{bd} (mV vs SCE)	i_{corr} (nA/cm^2)
Bulk	1	-900	-617	283	81
	2	-852	-537	315	53
	3	-847	-595	252	22
	Average	-866	-583	283	52
Weld	1	-753	-620	133	24
	2	-694	-588	106	65
	3	-780	-669	111	45
	Average	-742	-626	117	45
HAZ	1	-847	-586	261	79
	2	-812	-727	85	39
	3	-871	-567	304	71
	Average	-843	-627	217	63

Examples of 4 potentiostatic pitting measurements are shown for the 4 different areas in **Figure 17**. A python script was developed to count instances of metastable pits for all 12 measurements, and these results are summarized in **Table 6**. As seen in the table, 10 out of the 12 samples did not show any evidence of metastable pit events, and the only 2 that did exhibit metastable pitting came from the welded area of the plate. As such, the examples shown in Fig. 17a, 17c, and 17d demonstrate what the majority of the data for the potentiostatic pitting measurements looked like.

The plot for Fig. 17b comes from the measurement for Sample 1 of the welded area, which exhibited a metastable pit count of 35, and possible stable pitting after 36.2 hrs of the measurement (total of 60.2 hrs of immersion). This instance of possible stable pitting is shown in **Figure 18**. In this instance, the higher current was maintained for only 6 min before readjusting to baseline following the next readjustment of the OCP, so it is believed that the measurement technique influenced the pitting behavior and affected the results to some extent. This may indicate that for welded materials the OCP measurement, potentiostatic hold cycle times may need to be decreased.
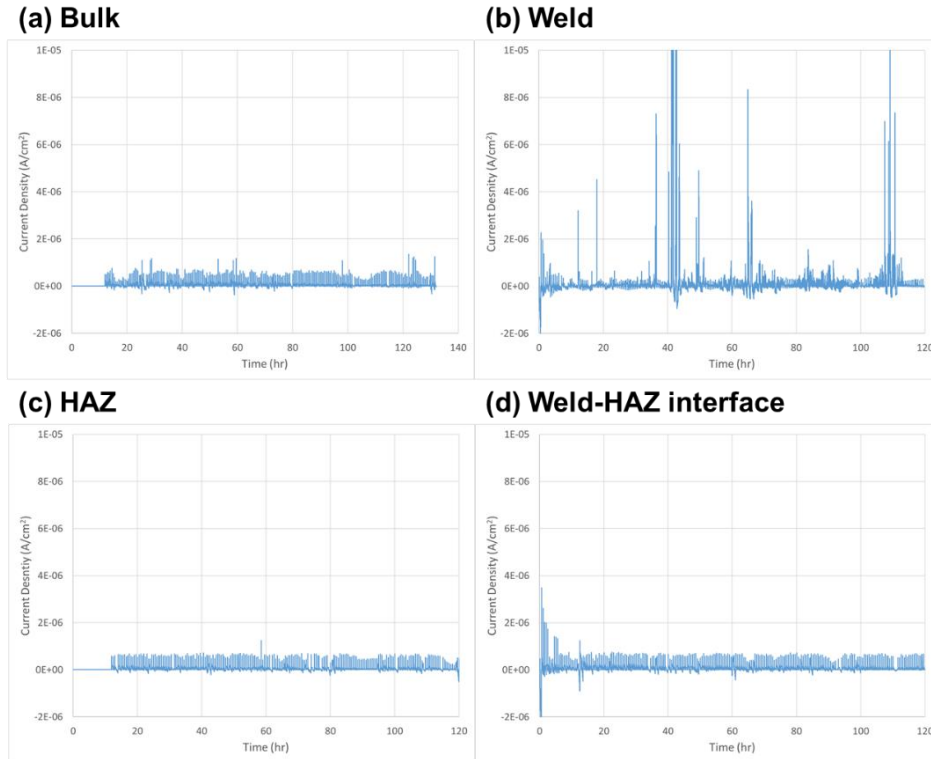
Figure 17. Example results of metastable pitting measurements for 4 samples from different areas of the welded plate: (a) bulk metal, (b) weld metal, (c) the heat-affected zone (HAZ), and (d) the weld/HAZ interface.
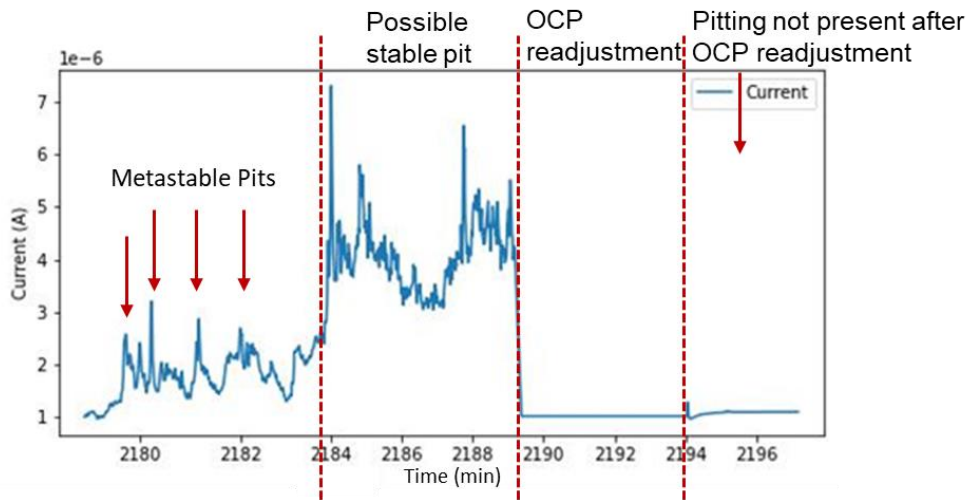
Figure 18. A subset of data from the potentiostatic pitting measurement of Sample 1 from the welded area of the plate. This subset shows a time period of metastable pitting involving into a more stable pitting current for a duration of 6 min. The OCP readjustment that occurs for 5 min every 25 min as part of this measurement shows afterward that this stable pitting event seems to have stopped.

Table 6. Summarized results of detecting metastable pit and stable pit events from the potentiostatic pitting measurements across 12 samples from different areas of the welded plate.

Area	Sample	Metastable Pit Count	Time to stable pitting (hr)
Bulk	1	0	n/a
	2	0	n/a
	3	0	n/a
Weld	1	35	36.4*
	2	2	n/a
	3	0	n/a
HAZ	1	0	n/a
	2	0	n/a
	3	0	n/a
Weld-HAZ Interface	1	0	n/a
	2	0	n/a
	3	0	n/a

*This time corresponds to a possible event of crevice corrosion, and the stable current lasted for 6 minutes before returning to baseline

The results of electrochemical measurements across different areas of the CMT welded AA5456 plate establish an apparent difference between the bulk and welded metal regions. From the OCP measurements, the welded area tended to exhibit more ennobled (more electropositive) potentials compared to both the bulk and HAZ regions, differing on average by slightly more than 100 mV, and this implicates possible galvanic couples between the weld and its surrounding area. Because the weld is more electropositive, a galvanic couple is likely to form where the weld acts as cathode to the HAZ or bulk as anode, meaning the latter regions may corrode and confer some protection to the welded region. Based on the intersection of the anodic polarization curves between these two regions, an expected galvanic corrosion current would likely be on the order of approximately 1 μA/cm^2, being of low enough magnitude that is likely not to cause serious risk to the surrounding area.

Of higher concern are the results related to pitting potentials and metastable pitting measurements. While the welded area is more ennobled, this higher OCP and slightly lower pitting potential means that the ΔE_{bd}, a characteristic which attests to susceptibility to pitting, is >150 mV lower on average compared to the bulk metal. This implies the welded region is more susceptible to pitting, and the metastable pitting measurements show that only the welded samples exhibited any evidence of metastable pitting and one instance of stable pitting after 36.4 hrs of immersion in ASTM SW. The metastable pitting data itself is somewhat consistent with results reported for AA5083 alloys by Gupta et al. [28], where the pitting rate is approximately <10/cm^2/min if ΔE_{bd} is on the order of 100 mV and decays towards zero as ΔE_{bd} increases above 200 mV. Still, one would expect higher metastable pit counts for all three welded samples during a five-day exposure, and this suggests the measurement itself may not have captured the expected behavior properly. It could be worthwhile to repeat these measurements with modified OCP-potentiostatic looping parameters using the potentiostat, smaller exposed surface areas, and

the use of a Faraday cage to eliminate interfering signals that could be affecting the recorded currents [28] [32].

The fact that the welded material shows clear differences in electrochemical response to the bulk and HAZ zone is attributable to changes in microstructure and surface state due to the CMT process. This is consistent with behavior encountered during corrosion testing of material welded using related GMAW processes. Immersion of aluminum alloys in seawater causes interactions with ions, most notably chloride (Cl^-), that can alter and destabilize the passive alumina (Al_2O_3) barrier, rendering the materials susceptible to localized corrosion [26] [27] [32] [33] [34]. Several factors influence this process, including pH, DO, salinity, temperature, and microstructure [26] [35], and this work in particular examined only effects pertaining to possible differences in the microstructure arising from the welding process. The literature on pitting of aluminum alloys attributes surface flaws and intermetallic particles formed with alloying constituents as the primary sites where pitting initiates [26] [27] [28] [32], with Fe- and Mg-incorporated intermetallic phases causing local galvanic couples that lead to corrosion in their vicinity. Extensive characterization would be necessary to confirm a change in the distribution of surface flaws and intermetallic phases, but the electrochemical data certainly indicates the CMT process alters the corrosion performance of the welded surface to slight detriment.

Keeping in mind these measurements only pertain to constant, quiescent immersion in ASTM SW at quiescent conditions, more work could be done to examine possible differences in corrosion performance of the bulk, HAZ, and welded surfaces under different environments of maritime concern: flowing immersion in seawater, alternate seawater immersion, salt spray, and atmospheric. Of these, alternate immersion and salt spray environments would be of higher priority due to the enhanced corrosivity from wet and dry cycles that can concentrate electrolytes in highly local areas [34]. Mitigation techniques such as coating or cathodic protection may be prudent for high-risk areas where this welding process is used.

6.   SUMMARY

This study evaluated the technical acceptability of welding with Fronius CMT technology as low, with significant risks for subsurface discontinuities such as lack of fusion when used for manual welding. The OEM of the welding equipment specifically cautioned against using Fronius CMT technology for applications involving material thicker than 0.125", noting that its very low heat input may make it unsuitable for such applications. Additionally, the OEM suggested using either PMC or a hybrid between CMT and PMC technology as an alternative to using pure CMT. However, at this time, the investigators are unable to evaluate these technologies appropriately due to a lack of experience with either PMC or mixed CMT/PMC processes, as well as a lack of appropriate welding equipment to conduct testing.

The as-welded mechanical properties are consistent with previous studies using GMAW technology. Fatigue properties of the CMT-welded material are consistent with existing test data for welding of grade 5456-H116 aluminum [30]. With regard to corrosion testing, the electrochemical measurements within this work indicate a possible performance risk due to the corrosion performance and thus service life of parts with CMT welds. However, the limited scope of electrochemical testing performed limits successful evaluation of risk at this time. Additional investigation under different possible service environments is required to fully assess the potential impacts of CMT welding with regard to maritime applications.

It should be noted that developmental solid-state repair techniques, such as cold spray or additive friction stir deposition, were specifically excluded from this review. These technologies fall outside the scope of this study, which focuses specifically on welding techniques. Although solid-state repair techniques offer unique advantages over traditional welding, particularly in surface engineering and related areas, they often require specialized equipment that is unlikely to be available at commercial ship repair facilities at present. Given the limited scope of this project, further exploration of these technologies is not included at this time.

In addition to the solid-state repair technologies noted above, consideration can be given to Severe Plastic Deformation (SPD) processes such as UIT and LSP, which deposit deep compressive stresses in the affected base material [1]. There is a potential for the use of SPD to reduce the likelihood of SCC in sensitized aluminum by imparting significant compressive stresses to the material surface, as SCC requires the presence of a sensitized microstructure, a corrosive environment, and sufficient tensile stresses. By eliminating tensile stresses using SPD, it is possible to avoid SCC in sensitized material. This technology area requires additional exploration, potentially as an adjunct to a future aluminum ship repair study.

While tests with Fronius CMT technology indicate that there are significant concerns with subsurface defects, there are alternative controlled waveform welding processes available. Fronius PMC technology, as previously discussed, is a potential candidate for low heat input welding of aluminum for maritime applications. In addition, exploration of non-arc welding technologies such as handheld laser welding is a potential option for future work.

This page intentionally left blank

1. REFERENCES

[1]   W. J. Golumbfskie, K. T. Tran, J. M. Noland, R. Park and D. J. Stiles, "Survey of Detection, Mitigation, and Repair Technologies to Address Problems Caused by Sensitization of Al-Mg Alloys on Navy Ships," *Corrosion,* vol. 72, no. 2, pp. 314-328, 2016.

[2]   I. N. A. Oguocha, O. J. Adigun and S. Yannacopoulos, "Effect of Sensitization Heat Treatment on Properties of Al-Mg Alloy AA55083-H116," Journal of Materials Science, vol. 43, pp. 4208-4214, 2008.

[3]   J. L. Searles, P. I. Gouma. and R. G. Buchheit, "Stress Corrosion Cracking of Sensitization AA5083 (Al-4.5Mg-1.0Mn)," Materials Sience Forum, Vols. 396-402, pp. 1437-1442, 2002.

[4]   A. J. Davenport, Y. Yuan, R. Ambat, B. Connolly, M. Strangwood, A. Afseth and G. Scamans, "Intergranular Corrosion and Stress Corrosion Cracking of Sensitized AA5182," Materials Science Forum, Vols. 519-521, pp. 641-646, 2006.

[5]   Alcoa, Inc., "Aluminum Steet and Plate in Marine Applications".

[6]   E. Bilgram and P. J. Walker, "Stress Corrosion Behavior and Welded Aluminum Alloy AlMg4.5Mn (5083)," in Third International Conference on Aluminum Weldments, 1985.

[7]   A. Saatchi, G. M. A. and M. R., "Evaluation of aluminum alloy 5083 weldments to stress corrosion cracking in seawater," INDUSTRIAL CORROSION AND CORROSION CONTROL TECHNOLOGY, p. 301, 1996.

[8]   S. Bond, "Corrosion of Welded Components in Marine Environments," in Prevention and Management for Marine Corrosion, London, 2003.

[9]   D3:7:2004, "Guide for Aluminum Hull Welding," American Welding Society, Miami, Fl, 2003.

[10]   "Welding Processes - Part 1, Chapter 4, Gas Metal Arc Welding," in Welding Handbook 9th ed., American Welding Society, 2004.

[11]   The Welding Institute, "MIG/MAG - Developments in Low Heat Input Transfer Modes," [Online]. Available: https://www.twi-global.com/technical-knowledge/job-knowledge/mig-mag-developments-in-low-heat-input-transfer-modes-133 . [Accessed 10 Jan 2022].

[12]   A. Pearce, "ESAB's Little Wonder Boxes Clever," Farmers Weekly, vol. 146, no. 2, p. 63, 2007.

[13]   EWM, "EWM Welding Processes - coldARC," [Online]. Available: https://www.ewm-sales.com/en/EWM_welding_processes/coldArc--82.html . [Accessed 13 Jan 2022].

[14]   Fronius, "CMT-Cold Metal Transfer: The Cold Welding Process for Premium Quality," [Online]. Available: https://www.fronius.com/en-us/usa/welding-technology/world-of-welding/fronius-welding-processes/cmt . [Accessed 13 Jan 2022].

[15]   Fronius, "Pulse Multi Control: Fronius has its Finger on the Pulse of Controlled and Fast Welding," [Online]. Available: https://www.fronius.com/en-us/usa/welding-technology/world-of-welding/fronius-welding-processes/. [Accessed 13 Jan 2022].

[16]   Kemppi, "Kemppi Special Processes," [Online]. Available: https://www.kemppi.com/en-US/offering/category/software/special-processes/ . [Accessed 13 Jan 2022].

[17]   Lincoln Electric, "Surface Tension Transfer (STT)," [Online]. Available: https://ch-delivery.lincolnelectric.com/api/public/content/38426f50886847f3a5253a3b6bee9e8b?v=4b065d51. [Accessed 13 Jan 2022].

[18]   Merkle, "ColdMIG," [Online]. Available: https://www.merkle.de/en/technologie/merkle-schweissverfahren/coldmig/. [Accessed 13 Jan 2022].

[19]   MIller, "Regulated Metal Deposition (RMD™) MIG Welding Process Improves Stainless Steel Pipe Fabrication," 2008. [Online]. Available: https://www.millerwelds.com/resources/article-

library/new-regulated-metal-deposition-rmd-mig-welding-process-improves-stainless-steel-pipe-fabrication. [Accessed 13 Jan 2022].

[20]   ASTM B928, "Standard Specification for High Magnesium Aluminum-Alloy Products for Marine Service and Similar Environments," ASTM International, West Conshohocken, PA, 2015.

[21]   AWS B4:0.2016, "Standard Methods for Mechanical Testing of Welds," American Welding Society, 2016.

[22]   ASTM E8-22, "Standard Test Methods for Tension Testing of Metallic Materials," ASTM International, West Conshohocken, PA, 2022.

[23]   ASTM D1141-98, "Standard Practice for Preparation of Substitute Ocean Water," ASTM International, West Conshohocken, PA, 2021.

[24]   A. S. Popernack, Loading Rate Effects on the Hydrogen Enhanced Cracking Behavior of Ni and Co-based Superalloys for Marine Applications, Master's Thesis, University of Virginia Department of Materials Science and Engineering, 2017.

[25]   J. Steiner, "Assessment of Corrosion Risk for Exposing UNS A95083 Alloy to Seawater Envionrments with Low Levels of Copper Contamination," NSWCCD Technical Report NSWCCD-61-TR-2022/5, 2022.

[26]   O. Nese, "Corrosion Properties of AA5083 and AA6082 in Seawater - Effect of Temperature, pH, and Potential," Master's Thesis Submitted to Norwegan University of Science and Technology, 2016.

[27]   M. Elboujdaini, M. T. Shehata and E. Ghali, "An Electrochemical Investigation And Corrosion Performance of Some Aluminum Alloys in Chloride Solution," Microstructural Science , vol. 26, 1998.

[28]   R. K. Gupta, N. L. Sukima, M. K. Cavanaugh, B. R. W. Hinton, C. R. Hutchinson and N. Birbilis, "Metastable Pitting Characteristics of Aluminum Alloys Measured Using Current Transitents During Potentiostatic Polarization," Electrochemica Acta, vol. 66, pp. 245-254, 2012.

[29]   T9074-AS-GIB-010/271, "Requirements for Nondestructive Testing Methods," NAVSEA Technical Publication, 1997.

[30]   A. Felker, "Compilation of 5xxx Series Mechanical Property Data from NSWCCD Technical Reports," Naval Surface Warfare Center, Carderock Division, unpublished.

[31]   M. E. McMahon, P. J. Steiner, A. B. Lass and J. T. Burns, "The Effect of Loading Orientation on the Stress Corrosion Cracking of Al-Mg Alloys," Corrosion, vol. 73, pp. 713-723, 2017.

[32]   A. R. Trueman, "Determining the Probability of Stable Pit Initiation on Aluminum Alloys Using Potentiostatic Electrochemical Measurements," Corrosion Science, vol. 47, pp. 2240-2256, 2005.

[33]   E. McCafferty, "Sequence of Steps in the Pitting of Aluminum by Chloride Ions," Corrosion Science, vol. 45, pp. 1421-1438, 2003.

[34]   F. C. Porter and S. E. Hadden, "Corrosion of Aluminum Alloys in Supply Waters," Journal of Applied Chemistry, vol. 3, pp. 385-409, 1953.

[35]   T9070-B1-DPC-010/630-1, "Ships Corrosion Control," NAVSEA Design Principles and Criteria Manual, 2021.

Test Plan Development and Reduction

A test plan was developed to identify and coordinate the required nondestructive and destructive testing. Four candidate base material and filler material combinations were identified for further work, although two of the proposed material combinations were eliminated near the end of the project due to workload constraints. The four combinations are identified as: (1) unsensitized grade 5456-H116 plate welded with grade 5556 filler material, (2) laboratory-sensitized grade 5456-H116 plate welded with grade 5556 filler material, (3) grade 6061-T6 plate welded with grade 4043 filler material, and (4) existing shipboard grade 5456-H116 plate welded with grade 5556 filler material. Note that combination (4), the shipboard plate, was obtained from existing specimens at NSWCCD from a decommissioned US Navy *Oliver Hazard Perry* class frigate. Unfortunately, due to resource constraints, combination (4) was not prepared or welded, and while combination (3) was prepared, tests were not performed.

The original test plan called for metallography, ASTM G67 NAMLTs, procedure qualification testing (bend tests and tensile tests), electrochemical testing, fatigue testing, and fracture toughness testing on both sensitized and unsensitized plates welded with the CMT process, as well as a limited amount of testing on the grade 6061-T651 plates. The original planned testing is listed in Table **7** below. However, due to constraints in funding as well as availability of test equipment, the planned testing was significantly downscoped. Testing of the grade 6061-T651 weldments was entirely omitted. Testing of unsensitized grade 5456-H116 aluminum welded with the CMT and GMAW processes was omitted. Testing of the sensitized aluminum plate welded with GMAW was omitted.

Table 7. Original test plan developed for this program.

Planned Testing												
	5456 (Unsensitized)				5456 (Sensitized)				6061			
Base Material	CMT		GMAW		CMT		GMAW		CMT		GMAW	
	Base	Weld	Base	Weld	Base	Weld	Base	Weld	Base	Weld	Base	Weld
Metallography Specimens	2	2	[1]	2	2	2	[1]	2	2	2	[1]	2
Bend Test Specimens	-	-	-	-	-	3	-	-	-	3	-	-
Tensile Test Specimens	-	-	-	-	-	2	-	-	-	2	-	-
G67 NAMLT	2	2	-	-	2	2	-	-	-	-	-	-
OCP + CYPOL	2	2	-	-	2	2	-	-	-	-	-	-
Potentiostatic Pol	5	5	-	-	5	5	-	-	-	-	-	-
Potentiostatic Pol (Mixed)	-	5	-	-	-	5	-	-	-	-	-	-
Fatigue (Air)	[3]	[3]	[3]	[3]	-	8	-	6	-	-	-	-
Fatigue (Seawater)	-	16	-	8	-	16	-	6	-	-	-	-
DC/PD Single-Edge Notch	-	-	-	-	-	2	-	-	-	2	-	[2]
[1] - Already performed on this base material.												
[2] - Obtained from existing test data.												
[3] - Unsensitized 5456 in air will have the same results as sensitized 5456.												

APPENDIX B:

Table 8. IMR Test labs AWS B4.0:2016 bend test results.

Sample	Result
AL22-11 BT1 - Root	No Cracking Observed
AL22-11 BT2 - Face	No Cracking Observed
AL22-11 BT3 - Root	No Cracking Observed
AL22-11 BT4 - Face	No Cracking Observed

Table 9. IMR Test Labs weld tensile test results.

Sample	Tensile Strength (ksi)	Max Load (lbs)	Failure Location
AL22-11 WT1	40.6	5255	Weld
AL22-11 WT2	41.5	5255	Weld

Table 10. Numerical fatigue data collected on lab-sensitized AA5456 weldments.

Specimen ID	Enviro.	Cyclic Load (lbs)	Stress (psi)	Cycles to Failure
A-1	Air	68.9	5000	29,547,000
A-2	Air	134.5	10000	1,168,000
A-3	Air	205.0	15000	709,000
A-4	Air	118.0	8500	15,242,000
A-5	Air	133.4	10000	14,695,000
A-6	Air	133.4	10000	10,452,000
A-7	Air	67.8	5000	13,029,000
A-8	Air	203.4	15000	672,000
S-1	Seawater	68.2	5000	14,258,000
S-2	Seawater	136.5	10000	1,575,000
S-3	Seawater	199.7	15000	237,000
S-4	Seawater	134.5	10000	536,000
S-5	Seawater	203.4	15000	179,000
S-6	Seawater	67.2	5000	6,943,000
S-7	Seawater	133.4	10000	735,000
S-8	Seawater	201.7	15000	338,000
S-9	Seawater	67.1	5000	11,556,000
S-10	Seawater	135.5	10000	1,913,000
S-11	Seawater	68.1	5000	14,630,000
S-12	Seawater	201.6	15000	160,000